

PM3 and DFT Quantum Mechanical Calculations of Two New N-Benzyl-5-Bromo Isatin Derivatives as Corrosion Inhibitors

Rehab Majed Kubba^{*1}, Mustafa Mohammed Kazem

¹Department of Chemistry, College of Science, Baghdad University, Baghdad, Iraq.

ABSTRACT

Theoretically two new derivatives of N-benzyl-5-bromoisatin namely N-benzyl-5-bromo-3-[(imine aceto) urea]-2-oxo indole (5BIO) and N-benzyl-5-bromo-3-[(imine aceto) thiourea]-2-oxo indole (5BIS) have been investigated as corrosion inhibitors for carbon steel surface in three media (vacuum, DMSO, and H₂O) using quantum mechanics calculations of the approximate semiempirical theory PM3 and Density Functional Theory DFT of (B3LYP) with a 6-311++G (2d,2p) by using Gaussian-09 program. The calculations of physical properties and quantum chemical parameters correlated to the inhibition efficiency all are studied and discussed at the equilibrium geometry at the three media. The results indicated that the two N-benzyl-5-bromoisatin derivatives could adsorb on the carbon steel surface firmly through the heteroatoms and through the 3-[(imine aceto) urea] for (5BIO) and 3-[(imine aceto) thiourea] for (5BIS), showing that the two inhibitors have excellent corrosion inhibition performance, and (5BIS) is a better corrosion inhibitor than (5BIO).

Keywords: PM3, DFT, Corrosion inhibitor, Isatin derivatives.

1. Introduction

Quantum chemical methods are particularly significant in the study of electrochemistry and provide researchers with a relatively quick way of studying the structure and behavior of corrosion inhibitors. Thus, it has become a common practice to carry out quantum chemical calculations in corrosion inhibition studies. The concept of assessing the efficiency of a corrosion inhibitor with the help of computational chemistry is to search for compounds with desired properties using chemical intuition and experience into a mathematically quantified and computerized form. Once a correlation between the structure and activity or property is found, any number of compounds, including those not yet synthesized, can be readily screened employing computational methodology [1] and a set of mathematical equations which are capable of representing accurately the chemical phenomenon under study [2,3]. DFT predicts a great variety of molecular features: the molecular weight structure, vibrational frequencies and atomization energies, ionization potential, magnetic properties, and the reaction path--- etc. [4,5]. Proven quantum chemical calculations to be a very powerful tool for the study of corrosion inhibition and take advantage of this mechanism studies [6-9]. Chemical concepts that are now used on a large scale and a description of the chemical reaction, electrical [10] hardness or softness amounts, etc., appear naturally in DFT [11]. The corrosion inhibitor is one of the most effective and economic methods important and most often used to protect the metal [12-14] including organic compounds containing heterogeneous atoms of unlinked electrons as nitrogen, sulfur, oxygen, and phosphorus [15]. The work of these organic compounds is to interact with the metal surface by adsorption. The importance of having polar functional groups as a reaction led to the stability of the adsorption process [16]. Isatin is one of a new class of molecules, not homogeneous with important and well tolerated in humans [17,18]. It can give different activities by entering groups to its ring. Isatin derivative is more effective compounds, and they are the most frequently used as corrosion inhibitors [19,20], including oxygen and amine, in addition to the aromatic ring, this could increase the ability of adsorption and for being a good inhibitor. There are a number of others mentioned parameters that must be involved, such as the effect of the solvent molecules, the nature of the surface, the absorption sites of metal atoms or oxide sites or vacant seats, competitive adsorption of various other chemical species in the liquid phase and solid [21]. The theoretical results obtained in this research are agreed very well with the experimental studies for carbon steel corrosion inhibition in 3.5% NaCl solution by the two newly prepared N-benzyl-5-bromoisatin derivatives [22]. The aim of this work is to study theoretically the parameters efficiency of corrosion inhibition of two newly prepared derivatives N-benzyl-5-bromo-3-[(imine aceto) urea]-2-oxo indole (5BIO) and N-benzyl-5-bromo-3-[(imine aceto) thiourea]-2-oxo indole (5BIS) Figure 1, which were chosen among many newly prepared derivatives of 5-bromoisatin [23] to be a good corrosion inhibitors theoretically, depending on studying their quantum mechanical inhibition efficiency parameters using the PM3 and DFT quantum mechanical methods.

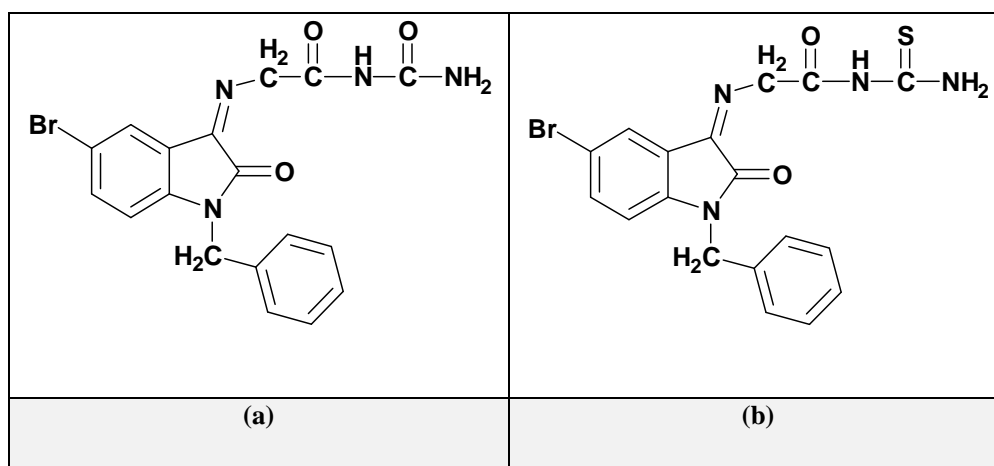


Figure 1-Chemical structure of **a**- N-benzyl-5-bromo-3-[(imine aceto) urea]-2-oxo indole, **b**- N-benzyl-5-bromo-3-[(imine aceto) thiourea]-2-oxo indole.

2.Results and Discussion

Molecular geometry

The construction of the two compounds was built using ChemDraw of Mopac program then equilibrium geometries were calculated by using Gaussian 09 package [24], their corresponding geometries in the gas phase were fully optimized using PM3 semiempirical method, then Density Functional Theory (DFT) was carried out using Becke's three-parameter functional and the correlation functional of Lee, Yang and Parr (B3LYP) with a 6-311++G (2d, 2p) level of theory [25-27] for calculating the geometries of the investigate molecules in three media (vacuum, aqueous and dimethyl sulfoxide), all at the same level of DFT theory. The final geometries of 5BIO and 5BIS according to the most correct method DFT are given in Figure 2.

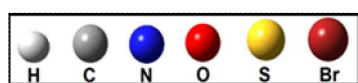
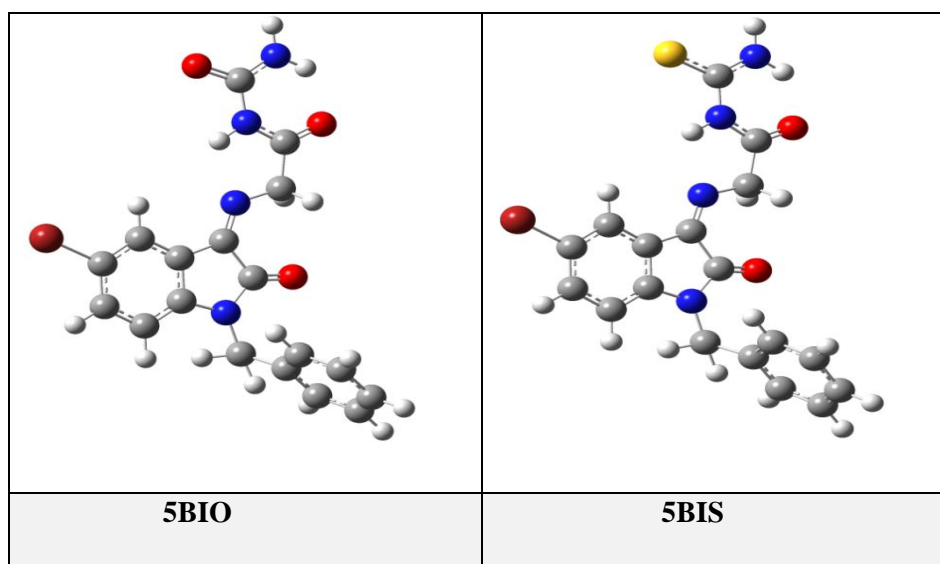


Figure 2-Equilibrium geometry of the inhibitors molecules calculated by DFT(B3LYP/6-311++G (2d,2p)) methods.

The substitution of carbonyl group C=O in 5BIO by thiocarbonyl group C=S in 5BIS made a difference observed in the computational results involves significant modifications on the structural parameters such as bond angles, and bond distances,

and dihedral angles of the studied inhibitors Table 1a,1b. Figure 3 shows the label of the atoms of the studied inhibitors. The optimized geometrical structures of 5BIO and 5BIS compounds are the same in the three media showing that the bond length of N1-C2, N1-C9, C2-C3, C3-C8, C5-Br, C6-C7, C15-O16, N17-C18 and C18-N20 bonds for 5BIO are longer than that for 5BIS by about (0.001-0.022) Å and most of the others in 5BIS are longer than that in 5BIO by about 0.001 Å. The longest bond length was observed for C18=S19 (1.667 Å) in 5BIS, and for C5-Br (1.915, 1.914 Å) in both 5BIO and 5BIS due to the large bulky volume of atoms S and Br compare to others. The compounds under investigation are not planar, it can be concluded that the adsorption on a metallic surface is clearly easy in addition to the values of the C2-N1-C10 for both 5BIO and 5BIS compounds Tables 1a,1b. The values of trans dihedral angles (N13C14C15O16, C14C15N17C18, C15N17C18O19, O16C15N17H) and cis dihedral angles (N13C14C15N17, O16C15N17C18, C15N17C18N20, O19C18N20H22) show that the molecule 5BIO and 5BIS are very close to being a planer in this part of the molecule. This result explains that the adsorption on the metallic surface was easier through these sites for 5BIS and for 5BIO. On using a solvent, for example (water, DMSO) there was no change in the bond length or bond angle.

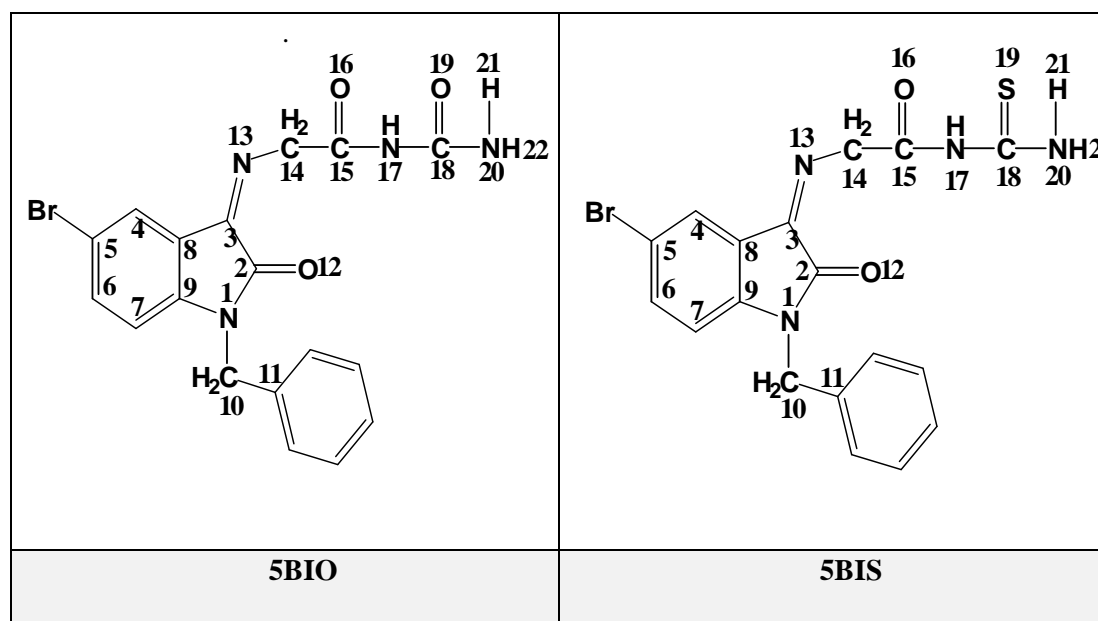


Figure 3-Label of 5BIO and 5BIS inhibitor compounds.

Table 1a-Calculated geometrical structure for 5BIO molecule by using DFT method.

Description Bond length	Bond length (Å)	Description angle (deg)	Angle (deg)	Description Dihedral angle(deg)	Dihedral angle (deg)
N1-C2	1.379G	C2N1C9	34.976G	H23N17C18O19	-0.085G
N1-C9	1.407G	C2N1C10	29.203G	C2N1C10C11	-113.037G
N1-C10	1.456G	N1C2C3	106.145G	C10N1C2O12	-178.004G
C2-C3	1.535G	N1C2O12	126.425G	O12C2C3N13	0.174G
C2=O12	1.213G	C2C3C8	105.225G	C2C3N13C14	0.082G
C3-C8	1.463G	C2C3N13	128.1288G	N13C14C15O16	179.863G
C3-N13	1.267G	C8C4C5	117.796G	N13C14C15N17	-0.102G
C4-C5	1.390G	C4C5C6	121.422G	C14C15N17C18	179.962G
C4-C8	1.385G	C4C5Br	119.349G	O16C15N17C18	-0.001G
C5-C6	1.390G	C6C7C9	117.914G	C15N17C18O19	179.927G
C5-Br	1.915G	C3C8C4	131.437G	C15N17C18N20	-0.074G
C6-C7	1.396G	N1C9C7	128.7111G	O19C18N20H21	-0.031G
C7-C9	1.383G	N1C9C8	110.231G	O19C18N20H22	-179.993G
N13-C14	1.450G	N1C10C11	114.411G	O16C15N17H	-179.988G
C14-C15	1.525G	C15N17H	116.247G		
C15=O16	1.222G	C3N13C14	121.979G		
C15-N17	1.364G	N13C14C15	112.821G		
N17-C18	1.418G	C14C15O16	119.717G		
C18=O19	1.216G	C14C15N17	115.412G		
C18-N20	1.349G	N17C18O19	119.134G		
N20-H22	1.003G	N17C18N20	115.193G		

Table 1b- Calculated geometrical structure for 5BIS molecule by using DFT method

Description Bond length	Bond length (Å)	Description angle (deg)	Angle (deg)	Description Dihedral angle(deg)	Dihedral angle (deg)
N1-C2	1.378G	C2N1C9	35.009G	C2N1C9C7	-179.742G
N1-C9	1.408G	C2N1C10	123.211G	C2N1C10C11	-111.036G
N1-C10	1.458G	N1C2C3	106.146G	C10N1C2C13	2.465G
C2-C3	1.535G	N1C2O12	126.516G	C12C2C3N13	0.261G
C2=O12	1.213G	C2C3C8	105.249G	C2C3N13C14	0.125G
C3-C8	1.463G	C2C3N13	128.096G	N13C14C15O16	-179.738G
C3-N13	1.267G	C8C4C5	117.773G	N13C14C15N17	0.200G
C4-C5	1.389G	C4C5C6	121.401G	C14C15N17C18	-179.788G
C4-C8	1.386G	C4C5Br	119.371G	O16C15N17C18	0.147G
C5-C6	1.391G	C6C7C9	117.929G	C15N17C18S19	179.883G
C5-Br	1.914G	C3C8C4	131.381G	C15N17C18N20	-0.058G
C6-C7	1.396G	N1C9C7	128.760G	S19C18N20H21	-0.057G
C7-C9	1.384G	N1C9C8	110.246G	S19C18N20H22	179.995G
N13-C14	1.449G	N1C10C11	114.347G	O16C15N17H	179.990G
C14-C15	1.524G	C18N20H21	117.726G		
C15=O16	1.221G	C3N13C14	122.022G		
C15-N17	1.369G	C13N14C15	112.581G		
N17-C18	1.395G	C14C15O16	120.082G		
C18=S19	1.667G	C14C15N17	115.101G		
C18-N20	1.337G	N17C18S19	119.479G		
N20-H22	1.003G	N17C18N20	115.691G		

3.Global molecular reactivity

Limits orbital theory is useful in predicting absorption inhibitor molecules responsible centers to interact with the metal [28]. Conditions that involve molecular orbital border (FMO) can provide the authoritarian contribution, due to the inverse of the energy dependence of the stability of the orbital energy difference ($\Delta E = E_{LUMO} - E_{HOMO}$). The energy HOMO (E_{HOMO}) refers to the ability to donate an electron to an acceptor, the molecule inhibitors with high values of E_{HOMO} have a tendency to donate electrons to the acceptor fitting with low energy molecular orbital empty. On the contrary, the energy LUMO (E_{LUMO}) refers to the ability to accept an electron of the molecule, which is the lowest value higher electron accepting capacity. The energy gap between the orbits of the border (ΔE) is another important factor in the description of the molecular activity, so when the energy gap decreased, improving the efficiency of the inhibitor [28]. Parameters Chemical quantum expense related to the efficiency of the inhibition of a molecule studied, such as molecular orbital (E_{HOMO}) highest occupied by electrons, and the energy of the lowest unoccupied molecular orbital (E_{LUMO}), the energy gap ($\Delta E = E_{LUMO} - E_{HOMO}$), the determination of the dipole moment (μ), and electronegativity (χ), and the effort ionization (IP), and electron affinity (EA), the global softness (S), and a part of electron transfer from the damper for the future (ΔN) of the inhibitor of iron particles, which have been compiled in tables (2a, 2b) and tables (3a, 3b, 4a, 4b) inhibitors with each PM3 and method of DFT.

According to the theory, Koopman in [29], the effort ionization (IE) and electronic affinity (EA) the HOMO energy is related to the ionization potential (IE) whereas the LUMO energy is linked to the electron affinity (EA), as follows:

$$IE \text{ (Ionization potential)} = -E_{HOMO} \quad (1)$$

IE is the amount of energy required for removing the electron of an atom. The low ionization energy gives high efficiency for inhibition.

$$EA \text{ (Electron affinity)} = -E_{LUMO} \quad (2)$$

EA is the amount of energy released when an electron is added to a neutral atom. The higher value of electron affinity means less stability and give high efficiency for inhibition.

Hardness (η) has been defined as the second derivative of the E. measures both the stability and reactivity of the molecule [30].

$$\eta \text{ (Hardness)} = (IE - EA) / 2 \quad (3)$$

$$\chi \text{ (Electronegativity)} = -\mu = (IE + EA) / 2 \quad (4)$$

This value is linked to HOMO and LUMO energy. The low value of electronegativity means high efficiency for inhibition. The global softness (S) is the inverse of the global hardness [31]. Softness from important properties to measure the molecular stability and reactivity

$$S \text{ (global softness)} = 1 / \eta \quad (5)$$

Global electrophilicity index (ω) introduced by Parr [32], a measure of the stabilization in energy after a molecule accepts an additional amount of electron. Good inhibitor with a lower value of global electrophilicity index.

$$\text{Global electrophilicity index } (\omega) = (-\chi)^2 / 2\eta \quad (6)$$

The fraction of electrons transferred (ΔN) from an inhibitor to carbon steel surface was also calculated using a theoretical χ_{Fe} and η_{Fe} values for mild steel of 7.0 eV mol^{-1} and 0.0 eV mol^{-1} , respectively [33]. The ΔN values are correlated to the inhibition efficiency according to Lukovits et al. study [34], the values of ΔN reported in Table 3b according to PM3 and Table 4b according to DFT; show that the 5BIS have the highest value of ΔN in the gas and two solvent phase. Therefore, the highest inhibition efficiency contemplates experimentally for 5BIS electrons flow from lower χ to higher χ until the chemical potentials become equal for example two systems, Fe, and inhibitor, are brought together, electrons will flow from an inhibitor to Fe. The (ΔN) was also calculated [35] by using the equation:

$$\Delta N \text{ (Electron transferred)} = (\chi_{Fe} - \chi_{inhib.}) / [2 (\eta_{Fe} + \eta_{inhib.})] \quad (7)$$

Where χ_{Fe} denote the absolute electronegativity of iron and $\chi_{inhib.}$ electronegativity of inhibitor molecule η_{Fe} and $\eta_{inhib.}$ denote the absolute hardness of iron and the inhibitor molecule respectively.

The dipole moment (μ in Debye) is another very important electronic parameter its product from uniform distribution charge on the atoms and the distance between the two bonded atoms [36]. High dipole moment values are reported to facilitate adsorption and therefore inhibition by influencing the transport process through the adsorbed layer the inhibition efficiency increases with dipole moments values [37,38]. The dipole moments of 5BIO and 5BIS are (4.4950, 6.2120 Debye), in the gas phase for PM3 method and (6.6832, 7.1186 Debye) for DFT method Tables (2a, 3a & 4a) respectively, increasing in dimethyl sulfoxide and aqueous solution. Metallic surface and these compounds probably indicate strong dipole-dipole interactions. The N-benzyl-5-bromoisatin derivatives adsorption in aqueous solution can be regarded as a quasi-substitution process of the DMSO and water molecules by the inhibitors molecules at the metal surface (H_2O ads). The higher value of the calculated μ and other parameters efficiency of the inhibitor molecule 5BIS enumerates its better inhibition efficiency than 5BIO in the gas phase and both solvents H_2O and DMSO at DFT calculations Tables 3a, 3b, 4a, 4b, even so PM3 calculations in the gas phase, Tables 2a, 2b. The calculated quantum chemical parameters in the presence of solvent (dimethyl sulfoxide, water) had shown a good effect for increasing the efficiency inhibition for 5BIO (Tables 3a, 3b), with slight decrease in efficiency inhibition for 5BIS (Tables 4a, 4b), but even though as a whole results, 5BIS has a better efficiency inhibition parameters in solvent than that of 5BIO inhibitor.

Table 2a- PM3 calculations for some physical properties of the inhibitor molecules at the equilibrium geometries.

Comp.	M. formula M. wt. (gm/mol)	ΔH_f^0 (kcal/mol) (kJ/mol)	E_{HOMO} (eV)	E_{LUMO} (eV)	ΔE HOMO-LUMO (eV)	μ (Debye)
5BIO	$C_{18}H_{15}N_4O_3Br$	-26.843	-9.1267	-1.3015	7.8251	4.4950
	415.257	-112.314				
5BIS	$C_{18}H_{15}N_4O_2SBr$	34.876	-8.8441	-1.4294	7.4147	6.2120
	431.317	145.922				

Table 2b-Quantum chemical parameters for the inhibitor molecules as calculated using PM3 method.

Comp.	IE (eV)	EA (eV)	η (eV)	χ (eV)	S (eV)	ω (eV)	ΔN
5BIO	9.1267	1.3015	3.9125	5.2141	0.2555	3.4743	0.2282
5BIS	8.8441	1.4294	3.7073	5.1368	0.2697	3.5587	0.2512

Table 3a- DFT calculations for some physical properties of the 5BIO inhibitor molecule in the three media (vacuum, DMSO, and H₂O) at the equilibrium geometries.

Inhib.	Sym.	E _{HOMO} (eV)	E _{LUMO} (eV)	$\Delta E_{HOMO-LUMO4}$ (eV)	μ (Debye)	E _{total} (eV)
5BIO (Gas)	C1	-6.6832	-3.1345	3.5487	6.6832	-101070.122
5BIO (DMSO)	C1	-6.4925	-2.9280	3.5644	7.8854	-101070.663
5BIO (H ₂ O)	C1	-6.4965	-2.9486	3.5479	8.6591	-101070.655

Table 3b-Quantum chemical parameters for the 5BIO inhibitor molecule in the three media (vacuum, DMSO, and H₂O) as calculated using DFT method.

Inhib.	IE (eV)	EA (eV)	η (eV)	χ (eV)	S (eV)	ω (eV)	ΔN
5BIO (Gas)	6.6832	3.1345	1.7743	4.9089	0.5635	6.7904	0.5892
5BIO (DMSO)	6.4925	2.9280	1.7822	4.7102	0.5610	6.2243	0.6423
5BIO (H ₂ O)	6.4965	2.9486	1.7739	4.7226	0.5637	6.2863	0.6418

Table 4a- DFT calculations for some physical properties of the 5BIS inhibitor molecule in the three media (vacuum, DMSO, and H₂O) at the equilibrium geometries.

Inhib.	Sym.	E _{HOMO} (eV)	E _{LUMO} (eV)	$\Delta E_{HOMO-LUMO}$ (eV)	μ (Debye)	E _{total} (eV)
5BIS (Gas)	C ₁	-6.0239	-3.1745	2.8493	7.1186	-109858.330
5BIS (DMSO)	C ₁	-6.4987	-2.9516	3.5470	8.6379	-109858.847
5BIS (H ₂ O)	C ₁	-6.4965	-2.9486	3.5479	8.6591	-109858.855

Table 4b-Quantum chemical parameters for the 5BIS inhibitor molecule in the three media (vacuum, DMSO, and H₂O) as calculated using DFT method.

Inhib.	IE (eV)	EA (eV)	η (eV)	χ (eV)	S (eV)	ω (eV)	ΔN
5BIS (Gas)	6.0239	3.1745	1.4246	4.5992	0.7019	7.4237	0.8425
5BIS (DMSO)	6.4987	2.9516	1.7735	4.7252	0.5638	6.2946	0.6413
5BIS (H ₂ O)	6.4965	2.9469	1.7739	4.7226	0.5637	6.2863	0.6418

Figure 4 shows the geometries optimization of compounds studied in the gas phase including LUMO and HOMO density distributions. It can be seen that the HOMO and LUMO distribution for both 5BIO and 5BIS are similar. HOMO mainly located on 3-[(iminoaceto) urea] indole -2-oxo moiety for 5BIO and for 5BIS the HOMO is mainly located at 3-[(iminoaceto) thiourea] indole -2-oxo moiety. The results suggest that the interaction between these molecules as an inhibitor with the surface of carbon steel is the same. Moreover, the distribution of electronic density of LUMO in both 5BIO and 5BIS are at the ring of isatin and at the aceto moiety.

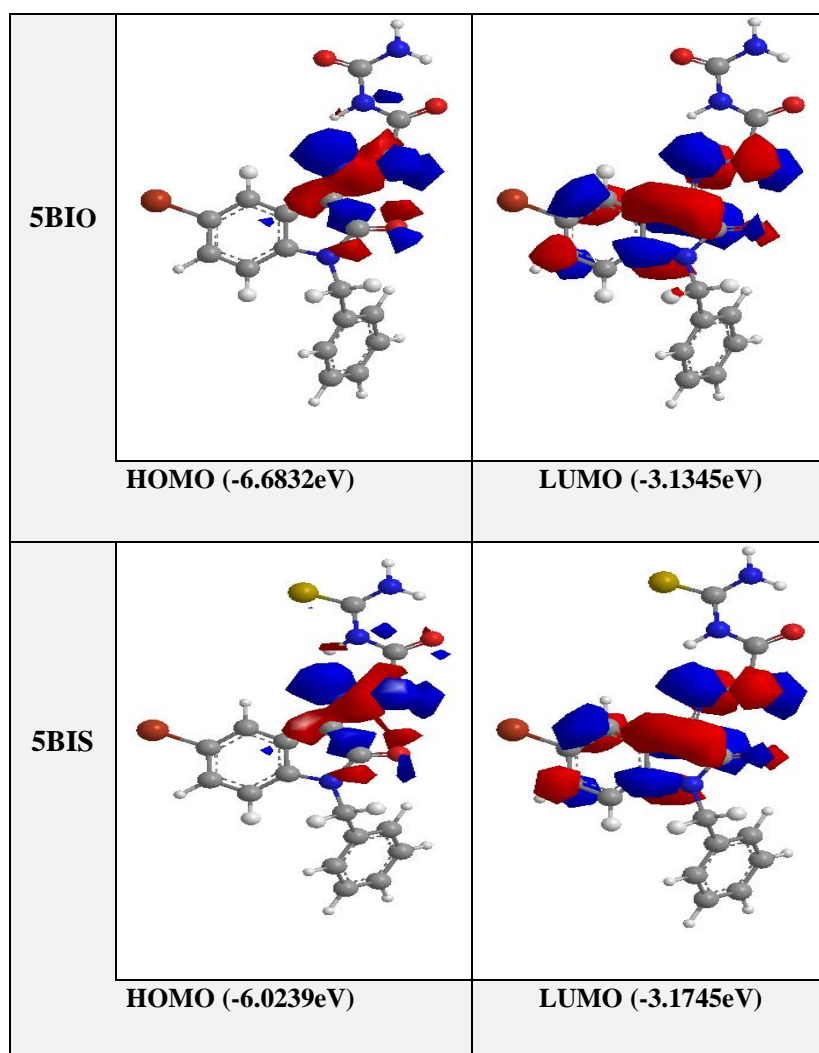


Figure 4- The Frontier molecule orbital density distributions of N-benzyl-5-bromo-3-[(imine aceto) urea]-2-oxo indole, and N-benzyl-5-bromo-3-[(imine aceto) thiourea]-2-oxo indole as calculations using DFT method. Red color indicates the negatively charged lobe, blue color indicates the positive charge lobe.

4. Local reactivity of the two N-benzyl-5-bromo isatin derivatives

The local reactivity of the studied inhibitors is investigated using the DFT Mulliken charges population analysis which is an indication of the reactive centers of molecules (nucleophilic and electrophilic centers). Therefore, the molecule regions where the electronic charge is large are chemically softer than the regions where the electronic charge is small, so the electron density plays an important role in calculating the chemical reactivity. Chemical adsorption interactions are either by electrostatic or orbital interactions. Electrical charges in the molecule considered driving force of electrostatic interactions. Proven charges are important in physicochemical properties of compound reactions [39,40].

For simplicity, only the charges on the nitrogen (N), oxygen (O), sulfur (S) and some carbon atoms are presented. Thus, the site for nucleophilic attack will be the place where the positive charge value is a maximum. In turn, the site for electrophilic attack was controlled by the negative charge value. Therefore, the favored sites for electrophilic attack and the most reactive of 5BIO are C10 and O12, N13, O16, N17, O19, N20 heteroatoms. For 5BIS, the most reactive sites are the same as for 5BIO, except S19 heteroatom instead of O19.

For the nucleophilic attack, the most reactive sites that can accept electrons for 5BIO are the same as for 5BIS and located at C9, C11 (which possess the highest positive charge on joining directly to the withdrawing aromatic ring) and C18 atoms which directly bonded to the nitrogen and sulfur atoms. These atoms accept electrons from 3d orbital's of the Fe atoms to form feedback bond, thus strengthening the interaction between inhibitor and Fe surface.

Based on the discussion above, it can be concluded that 5BIO and 5BIS have many active centers for adsorption on mild steel surface. Thus, the areas containing N, O and S atoms are the most favored sites for bonding to mild steel surface through donating electrons. However, the S atom can give and receive the electron to and from metal, respectively. The last process reinforces the inhibitor molecule adsorption on a metallic surface and the both process are more accentuated in 5BIS than in 5BIO. Taking into account the solvent effect, the electronic charge for the nucleophilic attack increases for 5BIO and 5BIS on C11 which is directly bonded to the aromatic ring from 0.849, 0.791 to 0.869, 0.813 in gas phase and solvents phase (DMSO and H₂O) respectively), and for C18 which is directly bonded to the oxygen and sulfur atoms. The electronic charge value of C18 site is 0.604: 0.516 in the gas phase and 0.640: 0.543 in solvents (DMSO and H₂O) respectively. For the electrophilic attack the electronic charge increases for 5BIS on S19 atom from -0.500 in the gas phase to (-0.604) in solvents phase (DMSO and H₂O) respectively. For 5BIO compound, the effect solvent on the electronic charge is more pronounced on O19 from (-0.496) in the gas phase to (-0.573) in solvents phase (DMSO and H₂O) Table 5. The electron donation from the metallic surface to inhibitor molecule is favored on many atoms in the aqueous phase for both 5BIO and 5BIS. The electronic charge values for electrophilic and nucleophilic attack of 5BIO and 5BIS are stronger in solution than in gas phase for C2, C3, C8, C11, C15 and C18 sites as a nucleophilic attack and for C5, Br, C7, C10, O12, N13, O16, O19 (5BIO), S19 (5BIS) and N20 sites as electrophilic attack. In solution, this function decreases for N1, C4, and C6 sites. From this analysis, it is obvious that in the aqueous solution, for 5BIS in addition to many atoms, the S atom is more likely to be a site for electrophilic attack in 5BIS at which it is absent in 5BIO and this leads to easy adsorption by donating electron from 5BIS to a metallic surface. Table 5 shows that the electronic charge of the electrophilic sites for both 5BIS and 5BIO increase slightly in the DMSO and aqueous solvents for about (0.01-0.10) on C2, C3, C11, C5, C18 and decreases about (0.02-0.04) on C8, C9, C14 atoms. The electronic charge for the nucleophilic sites of 5BIO decrease about (0.01-0.10) for N1, C4, C6, N17 atoms, and increase about (0.001-0.005) for C5, Br, C10, O16, while the electronic charge on atoms N13, O19, N20 increase about (0.10-0.06). Atoms with the highest negative charge have considered the role of electron donors when adsorption with metal surfaces.

The nucleophilic and electrophilic electronic charge values of 5BIO and 5BIS show that they are stronger in DMSO and H₂O solution than that in the gas phase making among adsorption by donating electron through sulfur atom for 5BIS which is more likely to be a site for the nucleophilic attack in DMSO and H₂O than in the gas phase.

Table 5-DFT Mulliken charges population analysis for the calculated inhibitor molecules 5BIO and 5BIS in the three media (vacuum, DMSO, and H₂O).

Atom	Electronic charge (ecu)	Electronic charge (ecu)	Atom	Electronic charge (ecu)	Electronic charge (ecu)
	5BIO	5BIS		5BIO	5BIS
N1	-0.055G	-0.045G	O12	-0.434G	-0.437G
	-0.026D	-0.017D		-0.499D	-0.500D
	-0.025W	-0.016W		-0.500W	-0.501W
C2	0.081G	0.047G	N13	-0.237G	-0.225G
	0.166D	0.132D		-0.244D	-0.233D
	0.168W	0.134W		-0.244W	-0.233W
C3	0.126G	0.110G	C14	0.171G	0.215G
	0.131D	0.118D		0.152D	0.192D
	0.131W	0.118W		0.152W	0.191W
C4	-0.195G	-0.160G	C15	0.094G	0.006G
	-0.189D	-0.161D		0.133D	0.050D
	-0.189W	-0.162W		0.133W	0.050W
C5	-0.114G	-0.101G	O16	-0.498G	-0.474G
	-0.129D	-0.114D		-0.555D	-0.523D
	-0.189W	-0.114W		-0.556W	-0.524W
Br	-0.044G	-0.041G	N17	-0.442G	-0.298G
	-0.061D	-0.060D		-0.430D	-0.286D
	-0.061W	-0.060W		-0.430W	-0.286W
C6	-0.409G	-0.425G	C18	0.604G	0.516G
	-0.378D	-0.392D		0.640D	0.543D
	-0.378W	-0.392W		0.640W	0.543W
C7	-0.211G	-0.186G	O19	-0.496G	-----
	-0.213D	-0.186D		-0.573D	
	-0.213W	-0.186W		-0.574W	
C8	0.277G	0.291G	S19	-----	-0.500G
	0.258D	0.270D			-0.596D
	0.253W	0.269W			-0.597W
C9	0.396G	0.371G	N20	-0.297G	-0.255G
	0.349D	0.319D		-0.313D	-0.262D
	0.348W	0.317W		-0.314W	-0.262W
C10	-0.264G	-0.231G			
	-0.292D	-0.263D			
	-0.293W	-0.263W			
C11	0.849G	0.791G			
	0.869D	0.813D			
	0.869W	0.813W			

G: gas phase, D: dimethyl sulfoxide (DMSO), W: water, blue color: increase in electronic charge to more positive, red color: increase in electronic charge to more negative

Based on the above results, it can be concluded that the two inhibitors have many functional centers for adsorption on carbon steel surface like (N, O, S) atoms and π electrons of the isatin ring which are donating electrons to carbon steel surface for bonding. However, the S atom can give and receive the electron from metal, because it has a lone pair of electrons and unfilled d orbitals. In addition, the active sites are the shape of 5BIS molecule is more planar than that for 5BIO. Tables 1a, 1b and Figure 5. This makes 5BIS to be adsorbed easier by donating electrons to the metallic surface [38].

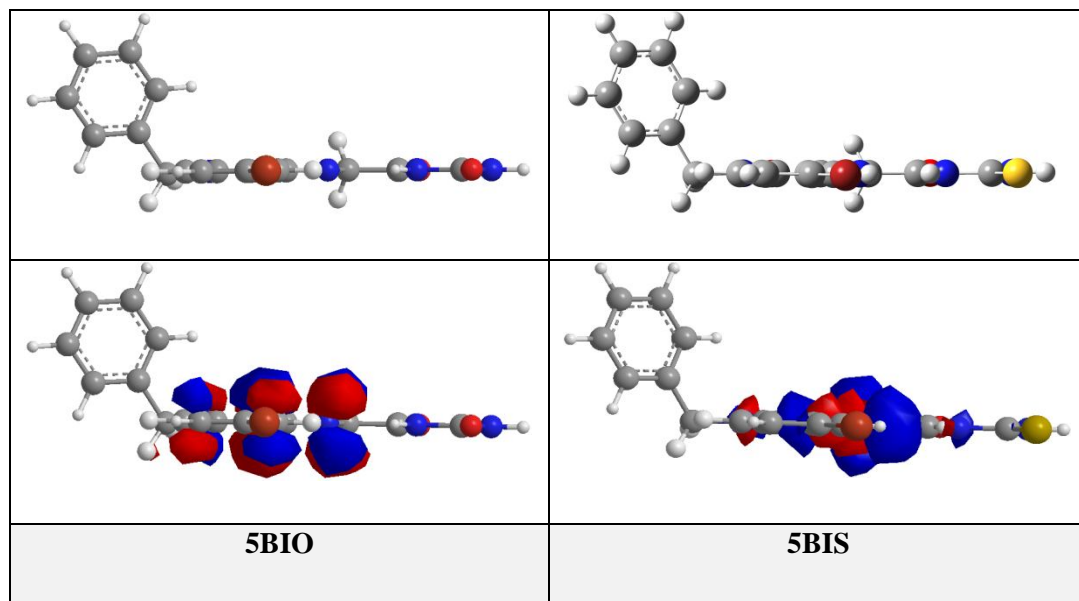


Figure 5- Surface area plane of the active sites of the calculated inhibitors.

5. Conclusion

1. Correlation related to the inhibition parameters calculated by quantum mechanical calculations PM3 and DFT (E_{HOMO} , E_{LUMO} , an energy gap ($\Delta E_{\text{HOMO-LUMO}}$), dipole moment (μ) ----etc., explained that the two inhibitor compounds can accept and donor electrons from the metal, and both could be adsorbed on carbon steel surface. The inhibition efficiency according to these parameters in the three media (vacuum, DMSO, and H_2O) were found to be increase in the order of ($\text{H}_2\text{O} > \text{DMSO} > \text{vacuum}$).
2. The theoretical studies revealed that the replacement of the thiourea group in 5BIS for the urea group in 5BIO promoted a decrease in the HOMO–LUMO energy gap and a significant increase in the dipole moment, which increased the corrosion inhibition efficiency. These results demonstrate the superiority of thiourea over urea as an organic corrosion inhibitor.
3. The density distributions of the frontier molecular orbital (HOMO and LUMO) showing that the adsorption of the two N-benzyl-5-bromo isatin derivatives occurs through the active centers of heteroatoms (nitrogen, oxygen, sulfur) and π electrons of the isatin ring and other heteroatoms which could be adsorbed on the carbon steel surface firmly through the heteroatoms (nitrogen, oxygen, sulfur) and π electrons of the isatin ring and through the 3-[(imine aceto) urea] for (5BIO) and 3-[(imine aceto) thiourea] for (5BIS), showing that the two inhibitors have excellent corrosion inhibition performance.
4. The geometrical structures in the three media (vacuum, DMSO, and H_2O) showed that the reactive sites of 5BIS molecule are slightly more planar than that for 5BIO, and this made 5BIS being more efficient as a corrosion inhibitor.

References:

- [1]. Karelson, M. and Lobanov, V. **1996**. Quantum chemical descriptors in QSAR/QSPR studies, *Chem. Rev.*, 96, pp: 1027–1043.
- [2]. Hinchliffe, A. **1994**. *Modelling Molecular Structures*. First Edition. John Wiley & Sons, New York.
- [3]. Hinchliffe, A. **1999**. *Chemical Modelling From Atoms to Liquids*. First Edition. John Wiley & Sons, New York.
- [4]. Von Barth, U. **2004**. Basic Density-Functional Theory. an Overview. *Physica. Scripta.*, (T109), pp: 9–39.
- [5]. Kubba, R.M. and Abdul-Sallam, A. **2013**. Quantum mechanical calculations of R-O thermal bond rupture energies in some ampicillin prodrugs. *Iraqi Journal of Science*, 54(4), pp: 739-752.
- [6]. Udhayakala, P., Jayanthi, A. and Rajendiran, T.V. **2011**. Adsorption and quantum chemical studies on the inhibition potentials of some formazan derivatives. *Der Pharma Chemica.*, 3(6), pp: 528-539.
- [7]. Ghailani, T., Balkhlima, R.A., Ghailani, R., Souizi, A., Tourir, R., Ebn Touhami, M. and Marakchi, K.N. **2013**. Experimental and theoretical studies of mild steel corrosion inhibition in 1 M HCl by two new benzothiazine derivatives. *Corrosion Science*, 76, pp: 317–324.
- [8]. Kandemirli, F.S. and Inc, S. **2007**. Theoretical study of corrosion inhibition of amides and thiosemicarbazones. *Corrosion Science*, 49, pp: 2118–2130.

- [9]. Mert, B.D., Mert, M.E., Kardas, G. and Yazıcı, B. **2011**. Experimental and theoretical investigation of 3-amino-1,2,4-triazole-5-thiol as a corrosion inhibitor for carbon steel in HCl medium. *Corrosion Science*, 53, pp: 4265–4272.
- [10]. Gece, G. **2008**. The use of quantum chemical methods in corrosion inhibitor studies. *Corrosion Science*, 50, pp: 2981–2992.
- [11]. Ahmad, I., Prasad, R. and Quraishi, M.A. **2010**. Thermodynamic electrochemical and quantum chemical investigation of some Schiff bases as corrosion inhibitors for mild steel in hydrochloric acid solutions. *Corrosion Science*, 52, pp: 933–942.
- [12]. Sonawane, R.P. and Tripathi, R.R. **2013**. The chemistry and synthesis of 1H-indole-2,3-dione (isatin) and its derivatives. *International Letters of Chemistry, Physics, and Astronomy*, 7(1), pp: 30-36.
- [13]. Bentiss, F., Lebrini, M. and Lagrenée, M. **2005**. Thermodynamic characterization of metal dissolution and inhibitor adsorption processes in mild steel/ 2,5-bis(n-thienyl)-1,3,4-thiadiazoles/hydrochloric acid system. *Corrosion Science*, 47(12), pp: 2915–2931.
- [14]. S_afak, S., Duran, B., Yurt, A. and Turkoglu, G. **2012**. Schiff bases as corrosion inhibitor for aluminium in HCl solution. *Corros. Sci.*, 54, pp: 251–259.
- [15]. Khalil, N. **2003**. Quantum chemical approach of corrosion inhibition. *Electrochim. Acta.*, 48(20), pp: 2635–2640.
- [16]. Choa, P., Liang, Q. and Li, Y. **2005**. Electrochemical, SEM/EDS and quantum chemical study of phthalocyanines as corrosion inhibitors for mild steel in 1mol/l HCl. *Appl. Surf. Sci.*, 252, pp: 1596-1607.
- [17]. Pakravan, P., Kashanian, S., Khodaei, M.M. and Harding, F.J. **2013**. Biochemical and pharmacological characterization of isatin and its derivatives: from structure to activity. *Pharmacological Reports*, 65, pp: 313-335.
- [18]. Al Maamari, K. **2013**. Isatin derivatives: synthesis, reactivity and anti corrosion properties. Ph.D. Thesis. Department of Chemistry, Faculty of Science, University of Mohammed-V-Agdal, Rabat.
- [19]. Parr, R.G. and Yang, W. **1989**. *Density Functional Theory of Atoms and Molecules*. First Edition. Oxford University Press, New York.
- [20]. Da Silva, J.F.M., Garden, S.J. and Pinto, A.C. **2001**. The chemistry of isatin: reviews from [1975 to 1999]. *J. Braz. Chem. Soc.*, 12(3), pp: 273-324.
- [21]. Fontana, M.G. and Staehle, K.W. **1970**. *Advances in Corrosion Science and Technology*. Second Edition. Volume 1. Plenum, New York.
- [22]. Al-Majidi S.M.H. and Hama, L.H.K. **2015**. Synthesis and antimicrobial evaluation activity of some new substituted spiro-thiazolidine, imidazolinone and azetidine derivatives of 5-bromo isatin, *Journal of Zankoi Sulaimani*, 17(1), pp: 49-59.
- [23]. Ahmed, H.J. **2015**. Synthesis, characterization and study of antimicrobial activity of some new Schiff base derivatives containing 5-bromo isatin moiety. M.Sc. Thesis. Department of Chemistry, College of Science, University of Baghdad. Baghdad, Iraq.
- [24]. Frisch, M.J., Trucks, G.W., Schlegel, H.B., Scuseria, G.E., Robb, M.A., Cheeseman, J.R., Montgomery, J.A., Jr., Vreven, T., Kudin, K.N., Burant, J.C., Millam, J.M., Iyengar, S.S., Tomasi, J., Barone, V., Mennucci, B., Cossi, M., Scalmani, G., Rega, N., Petersson, G.A., Nakatsuji, H., Hada, M., Ehara, M., Toyota, K., Fukuda, R., Hasegawa, J., Ishida, M., Nakajima, T., Honda, Y., Kitao, O., Nakai, H., Klene, M., Li, X., Knox, J.E., Hratchian, H.P., Cross, J.B., Bakken, V., Adamo, C., Jaramillo, J., Gomperts, R., Stratmann, R.E., Yazyev, O., Austin, A.J., Cammi, R., Pomelli, C., Ochterski, J.W., Ayala, P.Y., Morokuma, K., Voth, G.A., Salvador, P., Dannenberg, J.J., Zakrzewski, V.G., Dapprich, S., Daniels, A.D., Strain, M.C., Farkas, O., Malick, D.K., Rabuck, A.D., Raghavachari, K., Foresman, J.B., Ortiz, J.V., Cui, Q., Baboul, A.G., Clifford, S., Cioslowski, J., Stefanov, B.B., Liu, G., Liashenko, A., Piskorz, P., Komaromi, I., Martin, R.L., Fox, D.J., Keith, T., Al-Laham, M.A., Peng, C.Y., Nanayakkara, A., Challacombe, M., Gill, P.M.W., Johnson, B., Chen, W., Wong, M.W., Gonzalez, C. and Pople, J.A. **2009**. Gaussian 09, Revision E.01. Gaussian, Inc. Wallingford CT.
- [25]. Becke, A.D. **1993**. Density-functional thermochemistry. III. The role of exact exchange. *J. Chem. Phys.*, 98, pp: 5648-5652.
- [26]. Ee, C., Yang, W. and Parr, R.G. **1988**. Development of the Colle-Salvetti correlation-energy formula into a functional of the electron density. *Phys. Rev.*, B 41, pp: 785-789.
- [27]. Parr, R.G. and Yang, W. **1984**. Density functional approach to the frontier-electron theory of chemical reactivity. *Chem. Phys.*, 106, pp: 4049–4050.
- [28]. Issa, R.M., Awad, M.K. and Atlam, F.M. **2008**. Quantum chemical studies on the inhibition of corrosion of copper surface by substituted uracils. *Appl. Surf. Sci.*, 255(5), pp: 2433–2441.
- [29]. Koopmans, T. **1933**. Über die Zuordnung von Wellenfunktionen und Eigenwerten zu den einzelnen Elektronen eines Atoms. *Physica*, 1, pp: 104-113.
- [30]. Rauk, A. **2001**. *Orbital Interaction Theory of Organic Chemistry*. Second Edition. John Wiley & Sons: New York.
- [31]. Pearson, R.G. **1988**. Absolute electronegativity and hardness application to inorganic chemistry. *Inorganic Chemistry*, 27(4), pp: 734-740.

- [32].Parr, R.G. and Pearson, R.G. **1983**. Absolute hardness: companion parameter to absolute electronegativity. *J. Am. Chem. Soc.*, 105, pp: 7512-7516.
- [33].Chermette, H. **1999**. Chemical reactivity indexes in density functional theory. *J. Comput. Chem.*, 20,pp: 129-154.
- [34].Lukovits,I., Kálmán, E.and Zucchi, F.**2001**. Corrosion inhibitors-correlation between electronic structure and efficiency. *Corrosion*, 57, pp:3-9.
- [35].Wang, H., Wang, X., Wang, H., Wang, L. and Liu, A. **2007**. DFT study of new bipyrazole derivatives and their potential activity as corrosion inhibitors. *Journal of Molecular Modeling*. 13(1),pp: 147-153.
- [36].Zhao, P., Liang, Q. and Li, Y. **2005**. Electrochemical, SEM/ EDS and quantum chemical study of phthalocyanines as corrosion inhibitors for mild steel in 1 mol/l HCl. *Applied Surface Science*. 252(5),pp: 1596-1607.
- [37].Popova, A., Christov, M. and Deligeorgiev, T. **2003**. Influence of the molecular structure on the inhibitor properties of benzimidazole derivatives on mild steel corrosion in 1 M hydrochloric acid. *Corrosion*, 59,pp: 756–764.
- [38].Kubba, R.M.,and Abood, F.K. **2015**. Quantum chemical investigation of some Schiff bases as corrosion inhibitors for mild steel in hydrochloric acid solutions. *Iraqi Journal of Science*. 56(2B),pp: 1241-1257.
- [39].Stoyanova, A., Petkova, G.and Peyerimhoff, S.D. **2002**. Correlation between the molecular structure and the corrosion inhibiting effect of some pyrophtalone compounds. *Chem. Phys.*, 279, pp: 1-6.
- [40]. Li, X., Deng, S., Fu, H.and Li, T. **2009**. Adsorption and inhibition effect of 6-benzylaminopurine on cold rolled steel in 1.0 M HCl. *Electrochimica Acta.*, 54(16),pp: 4089-4098.